

Vibronic Structure of Jet-Cooled 2,6-Dimethylbenzyl Radical: Revisited

Gi Woo Lee and Sang Kuk Lee*

Department of Chemistry and The Chemistry Institute for Functional Materials, Pusan National University, Pusan 609-735, Republic of Korea

Received: September 26, 2005; In Final Form: December 1, 2005

We reexamined the vibronic structure of the jet-cooled 2,6-dimethylbenzyl radical that was generated from 1,2,3-trimethylbenzene seeded in a large amount of inert carrier gas helium using a pinhole-type glass nozzle in a corona excited supersonic expansion, from which the vibronically resolved emission spectrum was recorded with a long path double monochromator in the visible region. The spectrum exhibited bands arising from not only the $D_1 \rightarrow D_0$ transition but also the $D_2 \rightarrow D_0$ transition, in which transitions the accurate electronic energies of the D_2 and D_1 states and the revised vibrational mode frequencies in the ground electronic state were obtained by comparison with those from the known data of the precursor and an ab initio calculation.

Introduction

Whereas the benzyl radical, a prototype of the aromatic radical, has received much attention from spectroscopists, alkyl-substituted benzyl radicals have been less studied as large aromatic radicals.^{1–3} Earlier work on the xylyl radical in the visible region was published by Schuler et al.⁴ and by Walker and Barrow.⁵ Bindley et al.^{6,7} made vibronic assignments from an analysis of the emission spectra of xylyl radicals produced by an electric discharge of the corresponding xylenes.

Selco and Carrick⁷ analyzed the low-resolution vibronic emission spectra of xylyl radicals formed in a corona-excited supersonic expansion, in which several vibrational modes were identified. Charlton and Thrush⁸ obtained the first laser-induced fluorescence spectra of methyl substituted benzyl radicals and measured the lifetime in the excited vibronic states. Lee and colleagues^{9–11} extended the assignments of vibrational modes of xylyl radicals from the vibronic emission spectra. Recently, controversial assignments of *p*-xylyl radicals were resolved by an analysis of the vibronic band shapes from high-resolution emission spectra.¹² The torsional barrier of the internal methyl group was well determined for the xylyl radicals by Lin and Miller¹³ from the laser-induced fluorescence excitation and dispersed emission spectra. Recently, Lee's group presented the first vibronic emission spectra¹⁴ of the 2,6-dimethylbenzyl radical generated from 2,6-dimethylbenzene chloride using a technique of corona excited supersonic expansion. However, due to the insufficient S/N of the spectra, the assignment given to the transition was not very clear.

Supersonic free jet expansion has been known as a powerful spectroscopic technique for the observation of molecular spectra in the gas phase.¹⁵ The spectral simplification and stabilization of transient species associated with the expansion of inert carrier gas cannot be obtained in any other way. The combination of the supersonic expansion technique with emission spectroscopy has had an enormous influence on the repertoire of spectroscopic studies of molecular species in the gas phase. Of the emission sources developed for these purposes, the prospective one providing enough continuous photon intensity for high-resolution

studies of weak transition is the pinhole-type glass nozzle,^{16,17} which has been employed for observation of the vibronic emission spectra of transient molecules.¹⁸ This nozzle has been applied to the vibronic emission spectra of many jet-cooled benzyl-type radicals in the gas phase.^{19–21}

In this paper, we report the formation of the jet-cooled 2,6-dimethylbenzyl radical from 1,2,3-trimethylbenzene in a corona excited supersonic expansion using a pinhole-type glass nozzle, having observed the spectrum with the improved S/N, unlike our previous work, in which 2,6-dimethylbenzyl chloride was employed as a precursor. From an analysis of the spectrum, the electronic energies of the D_1 and D_2 states and the vibrational mode frequencies in the ground electronic state were obtained by comparison with those from both an ab initio calculation and the precursor.

Experimental Section

The 2,6-dimethylbenzyl radical was generated and vibronically excited using a technique of corona excited supersonic expansion, for which the experimental apparatus is similar to those described elsewhere.²² Briefly, it consists of a pinhole-type glass nozzle coupled with a high voltage dc discharge, a portable six-way cross-type Pyrex expansion chamber, and a spectrometer for observation of the vibronic emission spectrum.

The radical was generated and vibronically excited in a jet by the corona discharge of the 1,2,3-trimethylbenzene seeded in a large amount of inert carrier gas He. The concentration of the precursor in the carrier gas of about 2 bar was adjusted for the maximum intensity monitored in emission from the strongest band and believed to be about 1% in the gas mixture. The gas mixture was expanded, through the 0.4 mm diameter of the pinhole-type glass nozzle constructed in this laboratory, according to the method described previously.²³ The sharpened long tungsten rod acting as an anode was connected to the high voltage dc power supply in the negative polarity, in which the axial discharging current was 5 mA at 1500 V and stabilized using a $150 \times 10^3 \Omega$ current-limiting ballast resistor.

The Pyrex expansion chamber of six-way cross-type was made of thick-walled Pyrex tubes (Chemglass CG-138-02) of 50 mm in diameter. The chamber was evacuated by using a 800 L/min mechanical vacuum pump, resulting in the pressure

* Corresponding author. Fax: +82-51-516-7421. E-mail: sklee@pusan.ac.kr.

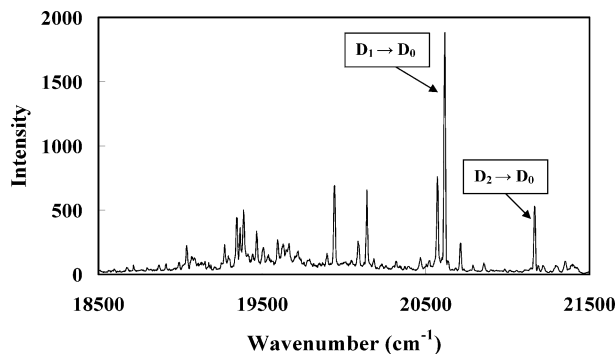


Figure 1. Portion of the vibronic emission spectrum of the jet-cooled 2,6-dimethylbenzyl radical in the $D_1 \rightarrow D_0$ and the $D_2 \rightarrow D_0$ transitions with the assignment. The weak bands around 19 400 cm^{-1} are from the well-known swan system of the C_2 that may be one of the most abundant fragments in the corona discharge of the hydrocarbon.

range $(1.0\text{--}2.0) \times 10^2$ Pa during continuous expansion with 2.0 bar of backing pressure. A cathode of a long copper rod was positioned to be parallel to the jet direction under the expansion chamber to avoid arcing noise reaching the spectrometer.

A blue-green colored jet was the evidence of the presence of the 2,6-dimethylbenzyl radicals in the expansion. The light emanating from the downstream jet area 5 mm away from the nozzle opening was collimated by a quartz lens ($f = 5.0$ cm) placed inside the expansion chamber and focused onto the slit of the monochromator (Jobin Yvon U1000) containing two 1800 lines/mm gratings and detected with a cooled photomultiplier tube (Hamamatsu R649) and a photon counting system. During the scans, the slits were set to 0.100 mm, providing a resolution of about 1.0 cm^{-1} in the visible region. The spectral region from 18 000 to 22 000 cm^{-1} was scanned at the step of 2.0 cm^{-1} over 2 h to obtain the final spectrum shown in Figure 1. The wavenumber of the spectrum was calibrated using the He atomic lines²⁴ observed in the same spectral region as the 2,6-dimethylbenzyl radical and is believed to be accurate within $\pm 1.0 \text{ cm}^{-1}$.

Because the 2,6-dimethylbenzyl radical has many vibrational modes and the assignments have not been completely confirmed, *ab initio* calculations on the ground electronic state were performed to assist the assignment of the vibronic bands. The calculations were executed with a personal computer equipped with an Intel Pentium 2.0 GHz processor and 512 MB RAM, and using the standard methods included in the Gaussian 98 program for windows package. The geometry optimization and vibrational frequency calculations were performed at the DFT level and the 6-311g* basis set was employed in all calculations.

Results and Discussion

Because methyl-substituted benzyl-type radicals have a planar structure with 7 delocalized π electrons, the electronic interaction between the methyl group and the benzene ring is undoubtedly of the second-order compared to that between the methylene group and the benzene ring, in which the methylene group contributes an electron. Thus, the electronic structure of the 2,6-dimethylbenzyl radical should exhibit a close relation to that of the benzyl radical, and one might be able to relate the two lowest lying electronic states of the 2,6-dimethylbenzyl radical to the parental benzyl $2^2B_2(D_2)$ and $1^2A_2(D_1)$ states.

The weak visible emission from the benzyl-type radicals is believed to arise from transitions to the $1^2B_2(D_0)$ ground state from the close-lying $2^2B_2(D_2)$ and $1^2A_2(D_1)$ excited states,² which can be mixed by vibronic coupling. Also, ring substitution

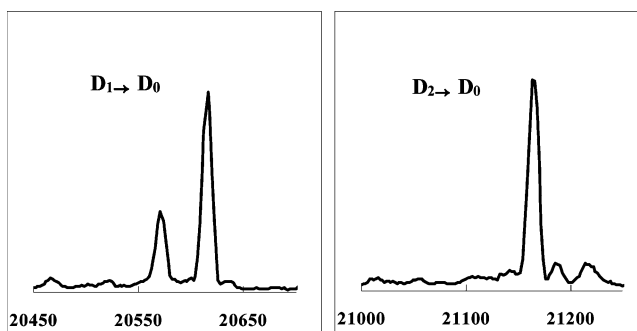


Figure 2. Observed band shapes of the origin bands of the $D_1 \rightarrow D_0$ and $D_2 \rightarrow D_0$ transitions. The difference cannot be clearly seen from the comparison because of the limited resolution of the spectrum.

is expected to affect the energies of the excited electronic states differently. Most of the benzyl-type radicals have the lowest excited electronic state of 1^2A_2 , except for the *p*-cyanobenzyl radical, which has that of 2^2B_2 .^{25,26}

Figure 1 shows a portion of the vibronic emission spectrum of the 2,6-dimethylbenzyl radical generated from the corona discharge of the precursor 1,2,3-trimethylbenzene in the visible region, in which many of the strong bands are observed with an excellent S/N in the region of 19 000–21 500 cm^{-1} . From the corona discharge of the precursor, two isomers, the 2,6-dimethylbenzyl and 2,3-dimethylbenzyl radicals, can be formed by extracting a hydrogen atom from the methyl group at the 2- and 1-positions of the precursor, respectively. The product was identified by comparison with the spectrum observed from that of the previous work, generated from 2,6-dimethylbenzyl chloride. The identification of each isomer was well demonstrated in the vibronic emission spectrum of the xylyl radicals by observing the origin band. The vibrational structure of the radical appears in the region within 2000 cm^{-1} from the origin band because the emission spectrum observed with a pinhole-type glass nozzle is similar to the dispersed fluorescence spectrum obtained by exciting the origin band of the electronic transition.^{27,28} Thus, the spacing of the vibronic bands from the origin band represents the vibrational mode frequencies in the ground electronic state.

It consists of two series of vibronic bands starting from the bands at 20 616 and 21 164 cm^{-1} , which are believed to be the origin bands of the $D_1 \rightarrow D_0$ and $D_2 \rightarrow D_0$ transitions, respectively, followed to lower energies by a series of vibronic bands. The absence of bands with observable intensity to the blue of the origin easily confirms the origin band because efficient vibrational relaxation can be obtained within the same electronic state during supersonic jet expansion.

Although the origin band of the $D_1 \rightarrow D_0$ transition of the 2,6-dimethylbenzyl radical was recently reported to be located at 21 164 cm^{-1} in the vibronic emission spectrum,¹⁴ the band shapes in Figure 2 show that the bands at 20 616 and 21 164 cm^{-1} should be reassigned as the origin bands of the $D_1 \rightarrow D_0$ and $D_2 \rightarrow D_0$ transitions, respectively, because the same vibrational structure in the ground electronic state as that of the $D_1 \rightarrow D_0$ transition was identified to the red region of the origin, due to the improved S/N of the spectrum. Thus we determined, for the first time, that the energy difference between the D_1 and D_2 states is 548 cm^{-1} in the 2,6-dimethylbenzyl radical, of which the separation is not sufficient to produce efficient vibronic coupling between the two adjacent excited electronic states,²⁹ as shown in Figure 3.

Because the 2,6-dimethylbenzyl radical belongs to the C_{2v} point group, the bands observed in this study should exhibit

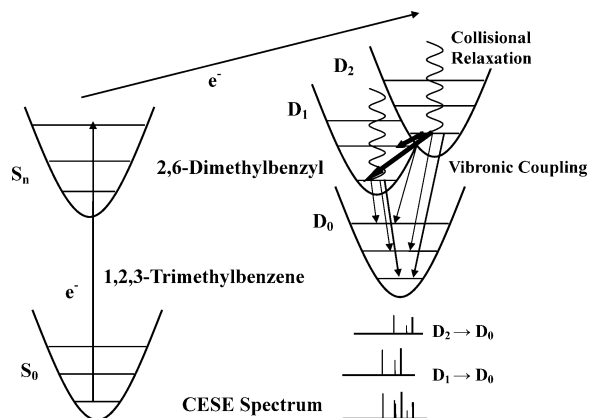


Figure 3. CESE diagram for observation of the visible vibronic emission spectrum of the 2,6-dimethylbenzyl radical generated from the corona discharge of 1,2,3-trimethylbenzene. The diagram represents the strong and moderate intensity from the $D_1 \rightarrow D_0$ and the $D_2 \rightarrow D_0$ transitions, respectively, due to the moderate vibronic coupling between the two adjacent excited electronic states.

TABLE 1: List of the Vibronic Bands Observed and Their Assignments

position ^a	intensity	spacing	assignments
21 164	s	0 ^b	origin band (0_0^0) (D_2)
20 714	w	450 ^b	$18b_1^0$ (D_2)
20 616	vs	548, ^b 0 ^c	origin band (0_0^0) (D_1)
20 140	s	476 ^c	$6a_1^0$
19 944	s	672 ^c	1_1^0
19 386	w	1230 ^c	$20a_1^0$
19 348	w	1268 ^c	13_1^0
19 040	w	1576 ^c	$8a_1^0$

^a In units of wavenumber (cm^{-1}). ^b Spacing from the origin band of the $D_2 \rightarrow D_0$ transition (21 164 cm^{-1}). ^c Spacing from the origin band of the $D_1 \rightarrow D_0$ transition (20 616 cm^{-1}).

the a- or b-type band shape, depending on the vibrational modes. Other types of benzyl radicals with the same symmetry show distinguishable band shapes in the emission spectra. The band shapes of the *p*-xylyl radical cleared the controversial assignments of the vibronic bands observed in the emission spectra. Also, the band shapes of many heavy molecules such as benzyl-type radicals have been analyzed to determine the direction of transition dipole moment by simulating the rotational contour of the bands observed.³⁰

Thus, the vibronic bands observed were assigned with the help of the known vibrational frequencies of 1,2,3-trimethylbenzene³¹ as well as those from an ab initio calculation. From the comparison between the two molecules, it seems clear that the vibrational structures in the ground electronic state of both molecules are well subject to isodynamic approximation, which is the correspondence of vibrational mode frequencies and transition intensity between molecules of similar structure. This

has already been applied to the vibronic assignments of many benzyl-type radicals.^{19–21} The vibronic bands observed in this study, together with the assignments, are listed in Table 1.

It has generally been accepted that calculation using the Gaussian 98 program at the DFT level with a 6-311g* basis set predicts the vibrational mode frequencies within, at most, $\pm 10\%$ of the experimental values. From the calculation for the 2,6-dimethylbenzyl radical, a total of 54 vibrational mode frequencies were obtained, of which 18, 8, 11, and 17 vibrational modes belong to the A_1 , A_2 , B_1 , and B_2 symmetries in the C_{2v} point group, respectively. The calculated values were multiplied by a scaling factor of 0.98 to match the observed values, as in most benzyl-type radicals. Table 2 lists the observed and calculated vibrational mode frequencies of the 2,6-dimethylbenzyl radical as well as those of the 1,2,3-trimethylbenzene,³¹ together with the symmetry of vibrational modes.

The strong bands at -476 cm^{-1} from the origin band, assigned to mode 6a of the C–C–C angle deformation vibration, respectively, are degenerate at 606 cm^{-1} in benzene. The splitting between 6a and 6b increases with the increasing size of the substituents. For the para-isomer, mode 6b has a higher frequency than mode 6a, but the trend is reversed for the ortho- and meta-isomers. The benzyl radical shows the 6a mode at 524 cm^{-1} whereas the 6b modes are observed at 615 cm^{-1} with stronger intensity.

The band at -450 cm^{-1} from the origin of the $D_2 \rightarrow D_0$ transitions was assigned to mode 18b of the C–CH₃ in-plane bending mode, because the observed intensity and frequency match those of the calculation. Modes 18a and 18b are also degenerate in benzene and are fairly insensitive to substitution. The counterpart mode, mode 18a, was not observed, because it is not active in 1,2,3-trisubstituted benzenes.³¹ Calculation showed that the frequency of the 18b component is higher than that of 18a in meta- and para-substitution, whereas in ortho-substitution the case is reversed.

One of the most important modes, mode 1 of ring breathing, was assigned to the strong band at -674 cm^{-1} from the origin band. The calculation and precursor showed excellent agreement with the observation. Also, the band shapes of this mode are very similar to others with the same symmetry. The weak band at -1230 cm^{-1} was assigned to mode 20a of C–CH₃ stretching vibration due to the coincidences with that of the precursor (1248 cm^{-1}) and the calculation (1218 cm^{-1}). In this mode, the precursor shows a very strong intensity in the Raman spectrum.

In our previous experiment, we observed several low frequency sequence bands regularly positioned in the vicinity of every strong vibronic band.¹⁸ The origin of the sequence bands is believed to belong to the combination bands associated with the excited vibrational state in the upper electronic state. Cossart-Magos and Cossart³⁰ assigned $16a_0^{11}1_1^0$, $18b_1^1$, 11_1^1 , and $10b_1^1$ for the bands observed at -11.3 , $+7.1$, -27.2 , and -54.8 cm^{-1} , respectively, from the origin band of the *p*-fluorobenzyl

TABLE 2: Vibrational Frequencies of the 2,6-Dimethylbenzyl Radical^a

mode ^b	this work (D_0)	previous work (D_0)	ab initio ^c B3LYP/6-311g* (D_0)	1,2,3-trimethylbenzene ^d (S_0)	symmetry (C_{2v})
origin ($D_2 \rightarrow D_0$)	21164				
origin ($D_1 \rightarrow D_0$)	20616	21164			
18b	450		445	459	a_1
6a	476	452	472	485	a_1
1	672		666	659	a_1
20a	1230		1218	1248	a_1
13	1268	1220	1267	1193	a_1
8a	1576		1581	1586	a_1

^a In units of wavenumber (cm^{-1}). ^b Reference 33. ^c Multiplied by a scaling factor of 0.98. ^d Reference 31.

radical in the $D_1 \rightarrow D_0$ transition. However, we could not assign the low-frequency sequence bands observed in this work because of the lack of vibrational data in the upper excited electronic states.

The several weak bands at approximately $19\,400\text{ cm}^{-1}$ are also from the well-known swan system of C_2 in the $A\ ^3\Pi_g-X'\ ^3\Pi_u$ transition, which is known to be one of the most abundant species in the decomposition fragments of hydrocarbons.³² With increasing discharge voltage, the intensity of the C_2 bands increases in the spectrum, whereas the intensity of the 2,6-dimethylbenzyl radical decreases significantly. Thus, the optimization of discharge condition is a crucial factor in the observation of vibronic emission spectrum.

In summary, the S/N of the vibronic emission spectrum of the 2,6-dimethylbenzyl radical was significantly improved by employing 1,2,3-trimethylbenzene as a precursor in a corona excited supersonic expansion. From the analysis of the spectrum, we identified several new bands arising from both the $D_1 \rightarrow D_0$ and the $D_2 \rightarrow D_0$ transitions, in which the electronic energies of the D_1 and the D_2 states were determined for the first time. The fact of the moderate-intensity transition from the D_2 state can be explained by the inefficient vibronic coupling between the two adjacent electronic states due to the small energy separation compared to that of the vibrational mode frequencies of the benzyl-type radicals.

Acknowledgment. This work was financially supported by the Korea Research Foundation, through Grant No. R14-2003-033-01002-0.

References and Notes

- (1) Cossart-Magos, C.; Leach, S. *J. Chem. Phys.* **1976**, *64*, 4006.
- (2) Selco, J. I.; Carrick, P. G.; *J. Mol. Spectrosc.* **1995**, *173*, 277.
- (3) Lin, T.-Y. D.; Tan, X.-Q.; Cerny, J.; Williamson, T. J.; Cullin, D.; Miller, T. A. *Chem. Phys.* **1992**, *167*, 203.
- (4) Schuler, H.; Reinbeck, L.; Kaberle, A. R. *Z. Naturforsch.* **1952**, *7A*, 421.
- (5) Walker, S.; Barrow, R. F. *Trans. Faraday Soc.* **1954**, *50*, 541.
- (6) Bindley, T. F.; Watts, A. T.; Watts, S. *Trans. Faraday Soc.* **1962**, *58*, 849.
- (7) Bindley, T. F.; Watts, A. T.; Watts, S. *Trans. Faraday Soc.* **1964**, *60*, 1.
- (8) Carlton, T. R.; Thrush, B. A. *Chem. Phys. Lett.* **1986**, *125*, 547.
- (9) Choi, I. S.; Lee, S. K. *Bull. Korean Chem. Soc.* **1995**, *16*, 1089.
- (10) Choi, I. S.; Lee, S. K. *Bull. Korean Chem. Soc.* **1996**, *17*, 749.
- (11) Choi, I. S.; Lee, S. K. *Bull. Korean Chem. Soc.* **1995**, *16*, 281.
- (12) Suh, M. H.; Lee, S. K.; Miller, T. A. *J. Mol. Spectrosc.* **1999**, *194*, 211.
- (13) Lin, T.-Y. D.; Miller, T. A. *J. Phys. Chem.* **1990**, *94*, 3554.
- (14) Lee, S. K.; Ahn, B. U.; Lee, S. K. *J. Phys. Chem. A* **2003**, *107*, 6554.
- (15) Miller, T. A. *Science* **1984**, *223*, 545.
- (16) Engelking, P. C. *Rev. Sci. Instrum.* **1986**, *57*, 2274.
- (17) Droege, A. T.; Engelking, P. C. *Chem. Phys. Lett.* **1983**, *96*, 316.
- (18) Engelking, P. C. *Chem. Rev.* **1991**, *91*, 399.
- (19) Lee, S. K.; Kim, Y. N. *J. Phys. Chem. A* **2004**, *108*, 3727.
- (20) Lee, S. K.; Kim, S. J. *Chem. Phys. Lett.* **2005**, *412*, 88.
- (21) Lee, S. K.; Lee, G. W. *Chem. Phys. Lett.* **2005**, *410*, 6.
- (22) Lee, G. W.; Seo, P. J.; Lee, S. K. *Bull. Korean Chem. Soc.* **2004**, *25*, 1459.
- (23) Lee, S. K. *Chem. Phys. Lett.* **2002**, *358*, 110.
- (24) Weise, M. L.; Smith, M. W.; Glennon, B. M. *Atomic Transition Probabilities*; NSRD-NBS4; NBS: Washington, DC, 1966.
- (25) Fukushima, M.; Saito, K.; Obi, K. *J. Mol. Spectrosc.* **1996**, *180*, 389.
- (26) Hiratsuka, H.; Mori, K.; Shizuke, H.; Fukushima, M.; Obi, K. *Chem. Phys. Lett.* **1989**, *157*, 35.
- (27) Lee, S. K.; Baek, D. Y. *Chem. Phys. Lett.* **1999**, *301*, 407.
- (28) Fukushima, M.; Obi, K. *J. Chem. Phys.* **1990**, *93*, 8488.
- (29) Lee, S. K.; Chae, S. Y. *Chem. Phys.* **2002**, *284*, 625.
- (30) Cossart-Magos, C.; Cossart, D. *Mol. Phys.* **1988**, *65*, 627.
- (31) Varsanyi, G. *Assignments for Vibrational Spectra of Seven Hundred Benzene Derivatives*; John Wiley & Sons: New York, 1974.
- (32) Pearse, R. W. B.; Gaydon, A. G. *The Identification of Molecular Spectra*, 4th ed.; Chapman and Hall: London, U.K., 1976.
- (33) Wilson, E. B. *Phys. Rev.* **1934**, *45*, 706.